graft polymerization of poly(MPTS), which could react with HAp crystals, at 70°C; (3) adsorption of HAp nanocrystals on the substrate and reaction with alkoxyl groups in the grafted polymer on the substrate at 80°C. In a cell adhesion test, it was confirmed that HUVEC adhered more plentifully on the HAp-coated substrate compared to the original one after only 4 h of initial incubation.

The calcinated HAp coating is effective way to obtain the affinity of cells, because it can coat metallic biomaterials without high-temperature post treatment. We fabricated a prototype of a stent made of the HAp-coated stainless steel (Fig. 6), and are now evaluating through animal implantation experiments *in vivo*.

5. Acknowledgment

This work was supported by a Research Grant for Cardiovascular Diseases from the Ministry of Health, Labour and Welfare, Japan.

6. References

1. Deligianni DD, Katsala ND, Koutsoukos PG, Missirlis YF: Effect of surface roughness of hydroxyapatite on human bone marrow cell adhesion, proliferation, differentiation and detachment strength. Biomaterials 22: 87-96, 2001
2. De Bruijn JD, Van Blitterswijk CA, Davies JE: Initial bone matrix formation at the hydroxyapatite interface in vivo. J Biomed Mater Res 29: 89-99, 1995.
3. Jarcho M: Calcium phosphate ceramics as hard tissue prosthetics. Clin Orthop 157: 259-278, 1981.
4. Jarcho M: Retrospective analysis of hydroxyapatite development for oral implant applications. Dent Clin North Am 36: 19-26, 1992.
5. Okumura M, Ohgushi H, Dohi Y, Katuda T, Tamai S, Tabata S (Nara Medical Univ., Nara, JPN), KOERTEN H. K: Osteoblastic phenotype expression on the surface of hydroxyapatite ceramics. J Biomed Mater Res 37: 122-129, 1997.
6. Aoki H, Medical Applications of Hydroxyapatite, Tokyo and St. Louis, Ishiyaku EuroAmerica Inc., 1994.
7. Furuzono T, Kishida A, Tanaka J. Nano-scaled hydroxyapatite/polymer composite I. Coating of sintered hydroxyapatite particles on poly(γ-methacryloxypropyl trimethoxysilane)-grafted silk fibroin fibers through chemical bonding. J Mater Sci: Mater Med 2004;15:19-23.
8. T. Furuzono, S. Yasuda, T. Kimura, S. Kyotani, J. Tanaka, A. Kishida, J Artif Organs 7 (2004) 137-144.
9. Furuzono T, Masuda M, Okada M, Yasuda S, Kadono H, Tanaka R, and Miyatake K, Increase of cell adhesiveness on poly(ethylene terephthalate) fabric by coating of sintered hydroxyapatite nanocrystals for development of an artificial blood vessel, ASAIO J, in contribution

10. Furuzono T, Wang P, Korematsu A, Miyazaki K, Oido-Mori M, Kowashi Y, Ohura K, Tanaka J, Kishida A. Physical and biological evaluations of sintered hydroxyapatite/silicone composite with covalent bonding for a percutaneous implant material. J Biomed Mater Res B: Appl Biomater 2003;65B:217-226.

11. Disegi JA, Eschbach L. Stainless steel in bone surgery. Injury 2000;31:2-6

12. Lau KW, Johan A, Sigwart U, Hung JS. A stent is not just a stent: Stent construction and design do matter in its clinical performance. Singapore Med J 2004;45:305-311

13. Kangasniemi IOM, Verheyen CCPM, van der Velke EA, deGoot, K, In vivo tensile testing of fluorapatite and hydroxyapatite plasma-sprayed coatings, J Biomed Mater Res, 28 (1994) 563-572

14. Ong JL, Lucus LC, Lacefield WR, Rigney ED, Structure, solubility and bond strength of thin calcium phosphate coatings produces by ion beam sputter deposition, Biomaterials, 13 (1992) 249-254

15. Yoshinari M, Hayakawa T, Wolke JCG, Influence of rapid heating with infrared radiation on RF magnetron sputtered calcium phosphate coatings, J Biomed Mater Res, 37 (1997) 60-67

16. Wang CK, Lin JHC, Ju CP, Ong HC, Chang RPH, Structural characterization of pulsed laser-deposited hydroxyapatite film on titanium substrate, Biomaterials, 18 (1997) 1331-1338

17. Kim DG, Shin MJ, Kim KH, Hanawa T, Surface treatments of titanium in aqueous solutions containing calcium and phosphate ions, Bio-Med Mater Eng, 9 (1999) 89-96

18. Mondragon-Cortez P, Vargas-Gutierrez G, Electrophoretic deposition of hydroxyapatite submicron particles at high voltages, Mater Lett, 58 (2004) 1336-1339

19. Wang Z, Chen F, Huang LM, Lin CJ, Electrophoretic deposition and characterization of nano-sized hydroxyapatite particles, J Mater Sci, 40 (2005) 4955-4957

20. Ong JL, Lucas LC, Post-deposition heat treatment for ion beam sputter deposited calcium phosphate coatings, Biomaterials, 15 (1994) 337-341

21. Weiss B, Stickler R, Phase instabilities during high temperature exposure of 316 austenitic stainless steel, Metal Trans, 3 (1972) 851-866

22. Filiaggi MJ, Pilliar RM, Interfacial characterization of a plasma-sprayed hydroxyapatite/Ti-6Al-4V implant system, in Transactions of the Tenth Annual Meeting of the Canadian Society for Biomaterials, pp.23-25 (1989)

23. Sonoda K, Furuzono T, Walsh D, Sato K, Tanaka J. Influence of emulsion on crystal growth of hydroxyapatite. Solid State Ionics 2002;151:321-327.

24. Okada M, Furuzono T, Nano-sized ceramic particles of hydroxyapatite calcined with an anti-sintering agent, J Nanosci Nanotech, in press

25. Okada M, Furuzono T, Highly dispersed rod-like nanocrystals of calcined hydroxyapatite fabricated by calcination with an anti-sintering agent surrounding the crystals, J Nanoparticles Res, in contribution

25. Zhang F, Kang ET, Neoh KG, Wang P, Tan KL, Surface modification of stainless steel by grafting of poly(ethylene glycol) for reduction in protein adsorption.

26. Nishizawa K, Toriyama M, Suzuki T, Kawamoto Y, Yokogawa Y, Nagata F, Chem Soc Jpn 1995;1:63

27. Brandrup J, Immergut EH (eds), Polymer Handbook, 3rd Edition, Wiley and Sons, Inc., New York, 1989

28. Mittal KL (ed), Silane and other coupling agents, Utrecht, VSP (1992)

29. Pluedemann EP (ed), Silane coupling agent, New York, Plenum Press (1991)

Table 1 Atomic percentages of the surfaces of the stainless-steel substrates evaluated by X-ray photoelectron spectroscopy

	C	O	Si	S	Cr	Fe	Ni
Original	25.9	50.9	0.6	0.4	10.6	5.0	1.0
Silized	35.0	44.4	2.5	1.9	9.3	5.0	0.6
Poly(MPTS)-Grafted	68.2	27.0	4.8	-	-	-	-

Figure captions

Fig. 1 Schematic model of the surface modification of stainless steel with hydroxyapatite nanocrystals

Fig. 2 ATR FT-IR spectra of poly(γ-methacryloxypropyl trimethoxysilane) prepared by solution polymerization (a) and the stainless steel substrate after the graft polymerization (b)

Fig. 3 SEM photographs of the surface of stainless steel after HAp modification followed by ultrasonic washing: (a) unmodified stainless steel; (b, c) PKBE-grafted stainless steel. (a, b) spherical HAp nanoparticles; (c) rod-like HAp nanoparticles

Fig. 4 SEM photographs of HUVEC adhering on the original (a), spherical HAp modified (b), and rod-like HAp modified (c) stainless steel after after incubation in 24-well multiplates (1 x 10^5 cells/well) at 37°C for 24 h.

Fig. 5 Type 316L stainless-steel stent before (a) and after (b) coating with HAp nanocrystals, and SEM photograph of the surface of the HAp-coated stent (c)

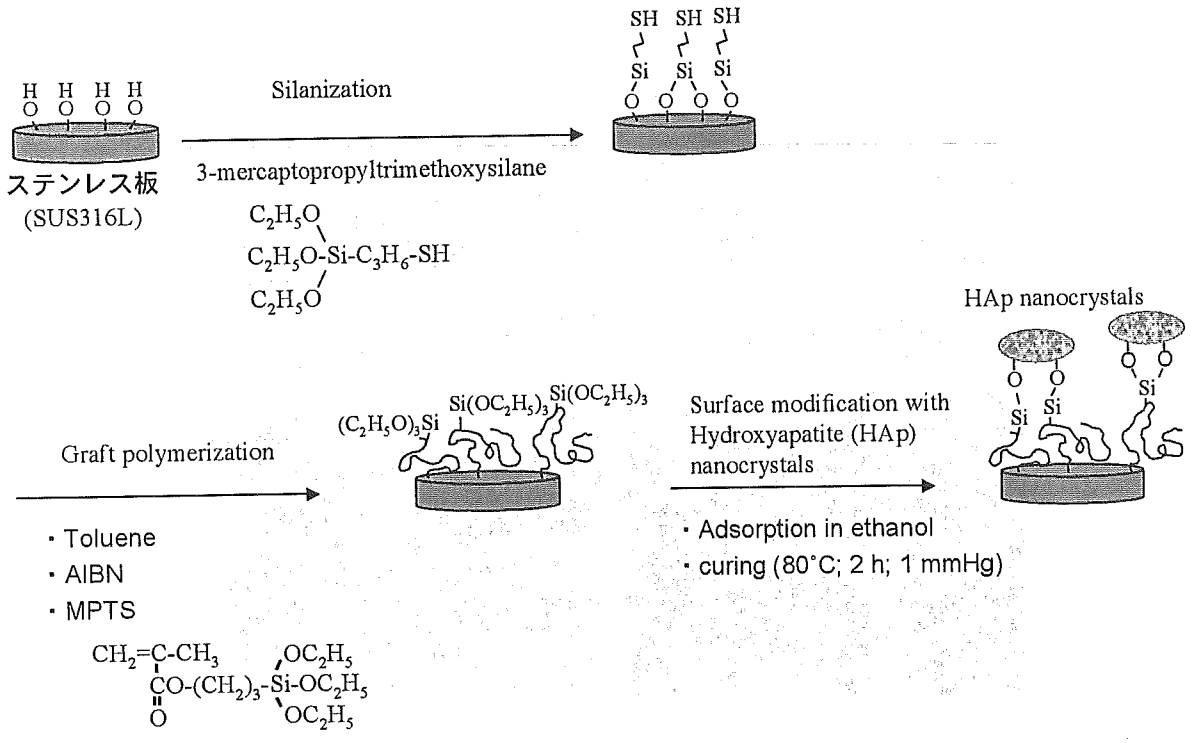

Fig. 1 Schematic model of the surface modification of stainless steel with hydroxyapatite nanocrystals

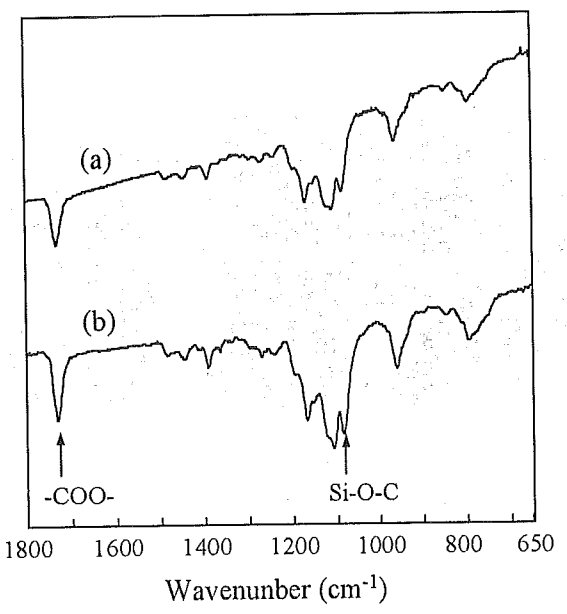

Fig. 2 ATR FT-IR spectra of poly(γ-methacryloxypropyl trimethoxysilane) prepared by solution polymerization (a) and the stainless steel substrate after the graft polymerization (b)

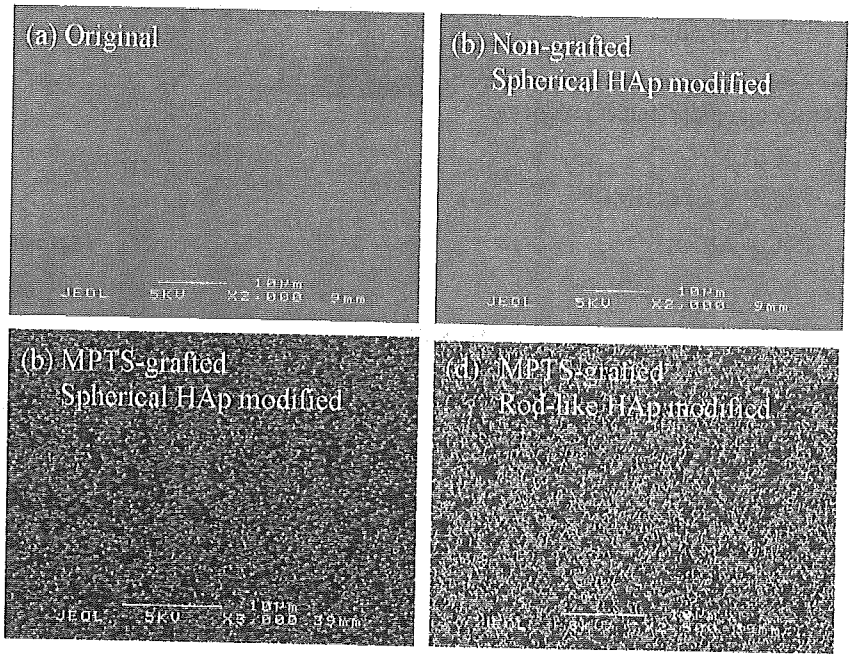

Fig. 3 SEM photographs of the surface of stainless steel after HAp modification followed by ultrasonic washing: (a) unmodified stainless steel; (b, c) PKBE-grafted stainless steel. (a, b) spherical HAp nanoparticles; (c) rod-like HAp nanoparticles

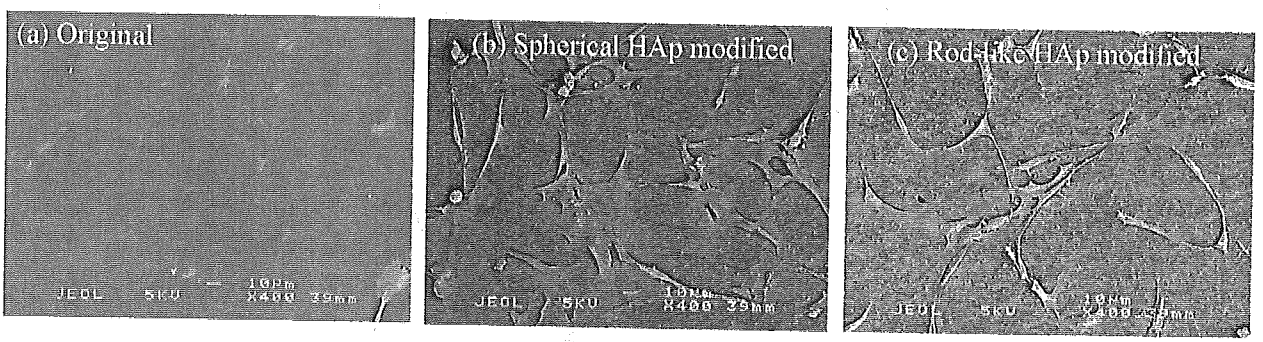

Fig. 4 SEM photographs of HUVEC adhering on the original (a), spherical HAp modified (b), and rod-like HAp modified (c) stainless steel after after incubation in 24-well multiplates (1×10^5 cells/well) at 37°C for 24 h.

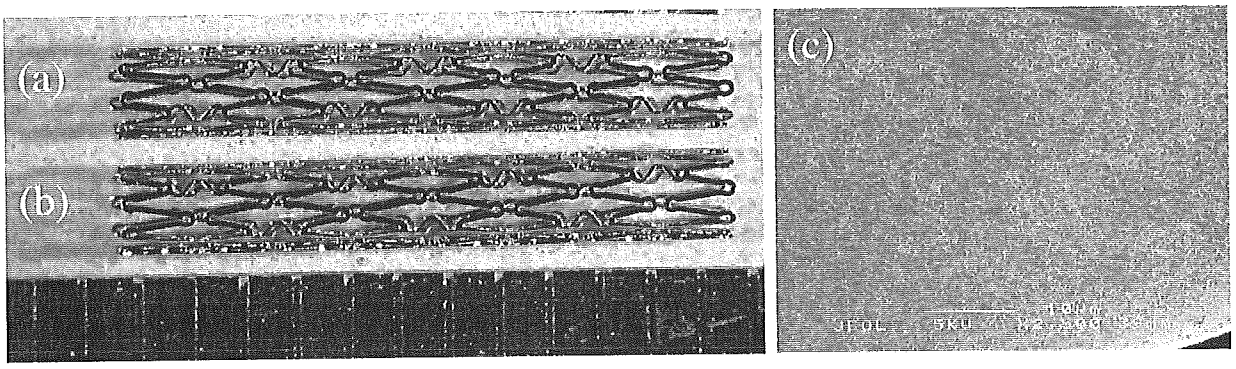

Fig. 5 Type 316L stainless-steel stent before (a) and after (b) coating with HAp nanocrystals, and SEM photograph of the surface of the HAp-coated stent (c)